Macromolecules
ARTICLE

Macromolecules **2009**, *42*, 6239–6244 **6239**
DOI: 10.1021/ma900922d

Thermosensitive Self-Assembly of Diblock Copolymers with Lower Critical Micellization Temperatures in an Ionic Liquid

Saki Tamura, Takeshi Ueki, Kazuhide Ueno, Koichi Kodama, and Masayoshi Watanabe*

Department of Chemistry & Biotechnology, Yokohama National University 79-5 Tokiwadai, Hodogaya-ku, Yokohama 240-8501, Japan

Received April 28, 2009; Revised Manuscript Received June 13, 2009

ABSTRACT: The aggregation behavior of diblock copolymers with lower critical micellization temperatures (LCMT) in an ionic liquid (IL) is presented for the first time. Poly(methyl methacrylate) (PMMA), poly(benzyl methacrylate) (PBnMA), and polystyrene (PSt) are known to be soluble, low-temperature-soluble and high-temperature-insoluble, and insoluble, respectively, in a typical hydrophobic IL, 1-ethyl-3-methylimidazoliumbis(trifluoromethane sulfonyl)imide. Well-defined thermosensitive diblock copolymers, consisting of PMMA as the first segment and PBnMA as the second, with different molecular weights and compositions were successfully prepared by atom transfer radical polymerization to yield P($BnMA_{2.2}$-*b*-MMA_{19}), P($BnMA_{7.3}$-*b*-MMA_{19}), and P($BnMA_{28}$-*b*-$BnMA_{41}$), where the numerals represent the number-average molecular weight of each segment (M_n/kDa). For comparison purposes, a thermo-insensitive diblock copolymer, consisting of PMMA and PSt (P($St_{1.7}$-*b*-MMA_{19})), was also prepared. The LCMT thermosensitivity and self-assembled behavior of the diblock copolymers in the IL were investigated in terms of the scattering intensity and hydrodynamic radius of the particles using the dynamic light scattering technique.

1. Introduction

The combination of macromolecules and ionic liquids (ILs) has recently been recognized to afford many possibilities for designing new polymeric materials.[1] From the perspective of practical applications, compatible combinations of polymers and ILs have been proposed for polymer electrolyte membranes,[2] separation membranes,[3] and catalyst supports[4] by utilizing the unique properties of ILs, such as their nonflammability, negligible volatility, high ion conductivity, and thermal and (electro) chemical stability. An understanding of the compatibility of polymers in ILs is crucial for designing such materials. Therefore, the estimation of the solubility parameters of ILs is a subject of intensive studies.[5] The solvent power of ILs can be tuned by designing the structure of cations and anions and choosing proper combinations of them.[6] For example, certain ILs show a surprisingly high solubility for poorly soluble biopolymers such as cellulose,[7] wool,[8] and silk.[9] All of these efforts imply that the combination of polymers and ILs has a fruitful future, which will bring new progress, challenges, and opportunities in polymer materials science.

We have been interested in the fact that certain polymers in ILs change their solubility in response to temperature. For example, poly(*N*-isopropylacrylamide) (PNIPAm), which exhibits a lower critical solution temperature (LCST) phase behavior in aqueous solutions,[10] also changes its solubility in an IL, but in a completely opposite manner. To elaborate, it exhibits an upper critical solution temperature (UCST) phase behavior in an IL.[11] In contrast, poly(benzyl methacrylate) (PBnMA) exhibits LCST phase separation in hydrophobic imidazolium-based ILs,[12,13] typically in 1-ethyl-3-methylimidazolium bis(trifluoromethane sulfonyl)imide ([C_2mim][NTf_2]). We also found that a chemically cross-linked PBnMA polymer network, i.e., PBnMA ion gel, shows discontinuous and reversible volume changes with a hysteresis loop, implying that it is the first-order transition.[12] It is also interesting to note that a neutral polymer network exhibits volume phase transition in an ionic solvent. Another LCST phase transition was also discovered for the combination of a polyether and an IL, and the full phase diagram of poly(ethyl glycidyl ether) in an IL was elucidated.[14]

Block copolymer self-assembly in selective solvents continues to be an active research area in polymer science.[15] Several research groups have reported block copolymer aggregation in ILs as solvents.[16] Lodge et al. investigated well-defined, systematically prepared polybutadiene−poly(ethylene oxide) (PB-*b*-PEO) block copolymer self-assembly in 1-butyl-3-methylimidazolium hexafluorophosphate ([C_4mim]PF_6).[16b] PB-*b*-PEO formed self-assembled structures consisting of micelles: insoluble dense PB cores surrounded by well-solvated PEO coronas. Cryogenic transmission electron microscopy (cryo-TEM) direct visualizations clearly revealed various nano-ordered self-assembled structures with universal morphologies such as spherical, cylindrical micelles and bilayer vesicles in an IL solvent.[16b] The basic idea of the self-assembly of a block copolymer in an IL medium has been expanded to physical ion gels,[17] thermoreversible ion gels,[18] a unique round-trip micellar shuttle between a hydrophobic IL and a phase-separated aqueous phase,[19] and the long-range-ordered regulation of ion paths by using polymer/IL composite films.[20]

Here, we focus on a novel class of stimuli-responsive diblock copolymers in an IL, which makes possible lower critical micellization temperature (LCMT) aggregation. Many studies on the LCMT aggregation behavior of micelles have been conducted in aqueous solutions.[21] Diblock copolymers having at least one segment with UCST thermosensitivity in an IL have been reported. However, no one has reported the LCMT thermosensitive self-assembly of systematically prepared diblock copolymers in an IL. A series of diblock copolymers, consisting of PBnMA and poly(methyl methacrylate) (P(BnMA-*b*-MMA)), were obtained by using well-established atom transfer radical polymerization (ATRP).[22] P(BnMA-*b*-MMA) can exhibit thermosensitive

*Corresponding author. E-mail: mwatanab@ynu.ac.jp.

Published on Web 06/26/2009

micellization in [C_2mim][NTf_2] above the LCMT aggregation temperature, based on the LCST solubility change of the PBnMA block and the completely compatible nature of the PMMA block[2a] in the IL. We applied the dynamic light scattering (DLS) technique to study the stimuli-induced micellization behavior of P(BnMA-*b*-MMA) in an IL. The results for the scattering intensity and hydrodynamic radius (R_h) of the block copolymers allowed us to explore the LCST thermosensitivity of the PBnMA segment by contrasting the results for those of a polystyrene−PMMA diblock copolymer (P(St-*b*-MMA)), which forms micelles irrespective of temperature in [C_2mim][NTf_2] due to the completely incompatible nature of the PSt segment in the IL. Furthermore, in order to elucidate how the molecular weight and composition affect the aggregation behavior of the diblock copolymers in the IL, we compared between the DLS results for a series of P(BnMA-*b*-MMA)s with different molecular weights and compositions.

2. Experimental Section

Chemicals. All of the chemical reagents used in this study were purchased from Wako, except for anisole (from Aldrich) and *N*,*N*,*N*′,*N*″,*N*″-pentamethyldiethylenetriamine (PMDETA) (from TCI). 1-Ethyl-3-methylimidazolium bis(trifluoromethane sulfonyl)imide ([C_2mim][NTf_2]) was synthesized and characterized according to a previously reported procedure.[23] MMA, St, and BnMA monomers were purified by distillation under reduced pressure over CaH_2 prior to use. CuBr was purified according to a previously reported procedure.[24] Other chemical reagents were used without further purification.

Synthesis of PMMA Macroinitiator. A PMMA macroinitiator was synthesized by ATRP.[22] CuBr (112 mg, 0.8 mmol), PMDETA (167 μL, 0.8 mmol), MMA (34 mL, 0.32 mol), and methyl 2-bromopropionate (90 μL, 0.8 mmol) were dissolved in 30 mL of anisole. The solution was degassed by three freeze−pump−thaw cycles. Polymerization was carried out at 60 °C for 2 h and was terminated by quenching with dry ice/methanol. The product was purified by reprecipitation using tetrahydrofuran (THF) as a good solvent and methanol as a poor solvent. The precipitate was dissolved in THF, and the solution was passed through a silica column (SiO_2) to remove the copper complex. The product was purified by reprecipitating again and was finally dried for 24 h at 80 °C under a vacuum condition. The structure of the polymer was characterized by ^{1}H NMR and gel permeation chromatography (GPC). The GPC was measured using THF as the eluent. The number-average molecular weight (M_n) and the polydispersity index (M_w/M_n, where M_w is the weight-average molecular weight) were measured using Tosoh columns calibrated by PMMA standards.

Synthesis of P(St-*b*-MMA) and P(BnMA-*b*-MMA)s. P(St-*b*-MMA) was synthesized by the ATRP method using the PMMA macroinitiator (Scheme 1). CuBr (38 mg, 0.25 mmol), PMDETA (52 μL, 0.25 mmol), St (5.0 mL, 43 mmol), and the PMMA macroinitiator (5.0 g, 0.25 mmol) were dissolved in anisole (20 mL). The solution was degassed three times by freeze−pump−thaw cycles, and polymerization was carried out at 100 °C for 45 h. The product was purified and characterized by the same procedure used for preparing the PMMA macroinitiator. P(BnMA-*b*-MMA)s were also prepared in a similar manner, except that BnMA was used as the monomer instead of St. For the polymerization of BnMA, the reaction was carried out at 75 °C for 2 h. M_w/M_n for the block copolymers were obtained from GPC measurements under the same conditions as in the case of the PMMA macroinitiator. M_n was calculated by combining the ^{1}H NMR of the diblock copolymers with the results of M_n from the GPC of the PMMA macroinitiator. The ^{1}H NMR charts and GPC traces for all of the polymers prepared here are available in the Supporting Information. The results of the polymer characterizations are shown in Table 1, where f_{BnMA} and f_{St} are respectively the volume fractions of BnMA and St in the block copolymers.

Table 1. Characterization of Polymers

	M_n/kDa	M_w/M_n	$f_{St,BnMA}$
$PMMA_{19}$	19	1.17	
P($St_{1.7}$-*b*-MMA_{19})	1.7−19	1.27	0.091
P($BnMA_{2.2}$-*b*-MMA_{19})	2.2−19	1.23	0.10
P($BnMA_{7.3}$-*b*-MMA_{19})	7.3−19	1.29	0.28
P($BnMA_{28}$-*b*-MMA_{41})	28−41	1.22	0.40

Scheme 1. Synthetic Procedure for PMMA Macroinitiator, P(St-*b*-MMA), and P(BnMA-*b*-MMA), Respectively

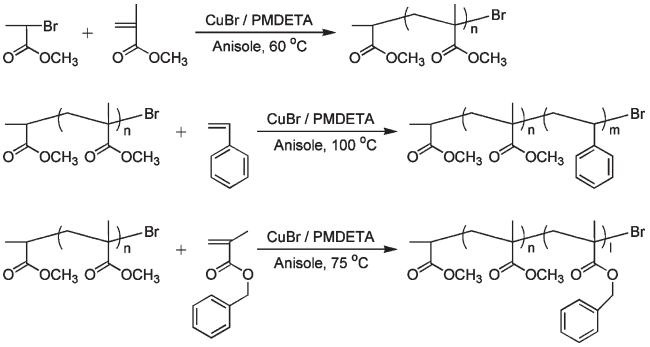

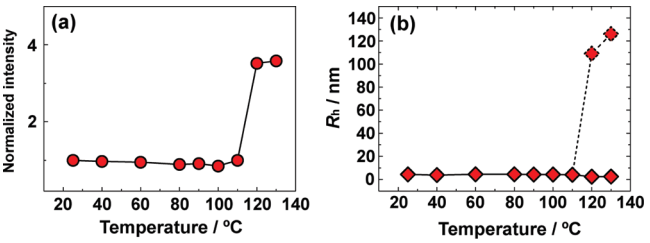

Figure 1. (a) Relationship between the normalized scattering intensity at a scattering angle of 90° and temperature for P($BnMA_{2.2}$-*b*-MMA_{19}) in [C_2mim][NTf_2] solution (2 wt %). The normalized intensity is defined as the intensity at each temperature divided by that measured at 25 °C. (b) Relationship between the R_h of P($BnMA_{2.2}$-*b*-MMA_{19}) in [C_2mim][NTf_2] and the temperature. Broken line indicates minor components in the system.

Dynamic Light Scattering. Polymer samples were dissolved into [C_2mim][NTf_2] by the cosolvent (THF) evaporation method.[12,13] DLS measurements were performed on an Otsuka Electronics DLS-6500 equipped with an ALV correlator and an Ar laser (488 nm). Experiments were performed at different temperatures (25−130 °C), and the correlation functions were recorded at various scattering angles between 20° and 120°.

The correlation functions were fitted using the cumulant or double-exponential function. The distribution function of R_h was also revealed by applying the inverse Laplace transformation to the correlation function through the well-established CONTIN program. The temperature dependency of the viscosity of [C_2mim][NTf_2] was calculated using the Vogel−Tammann−Fulcher (VTF) equation and the fitting parameters.[23b] The refractive index of [C_2mim][NTf_2] was obtained from previous reports.[13a]

3. Results and Discussion

Comparison between Thermosensitive and Thermoinsensitive Diblock Copolymers in an IL. Figure 1 shows the temperature dependency of the normalized scattering intensity and R_h for P($BnMA_{2.2}$-*b*-MMA_{19}) dissolved in [C_2mim][NTf_2] (2 wt %). The normalized scattering intensity was defined as the intensity at each temperature divided by the intensity measured at 25 °C. The scattering intensity of

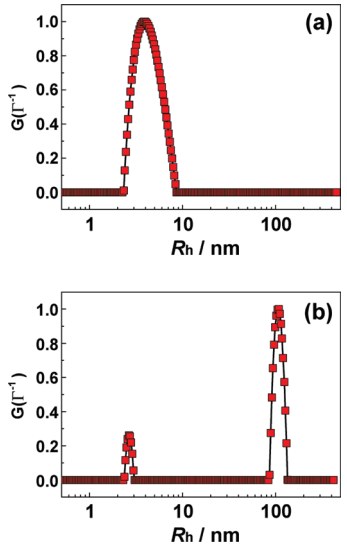

Figure 2. Distribution function of R_h for P(BnMA$_{2.2}$-*b*-MMA$_{19}$) (2 wt %) in [C$_2$mim][NTf$_2$] solution measured at (a) 25 and (b) 120 °C.

the diblock copolymer solution suddenly increased above 120 °C. The temperature at which the scattering intensity started to increase was slightly higher than that of the previously reported LCST phase separation temperature (105 °C) of PBnMA homopolymer with $M_n = 28.3$ kDa and $M_w/M_n = 2.76$.[12,13] The increased scattering intensity observed here was brought about by the fact that single polymer chains, P(BnMA$_{2.2}$-*b*-MMA$_{19}$), aggregated to form large size micelles. The R_h values of the particles were calculated from the cumulant fitting below the aggregation temperature but were calculated from the double-exponential fitting above this temperature, since the single polymer chains still remained, even above the aggregation temperature. The R_h values were found to be 4.4 nm at 25 °C from the cumulant fitting and 2.5 and 109 nm at 120 °C from the double-exponential fitting. The results of the CONTIN analysis at temperatures below and above the aggregation temperature (Figure 2) were also an evidence for the existence of the unimers. A small particle size, consistent with the size of a single polymer chain, could be seen at both 25 and 120 °C. It should be noted, from the distribution of the unimer particle size in Figure 2a,b, that the unimers were polydispersed at 25 °C but were sharply distributed at 120 °C. This implies that single polymer chains with relatively higher molecular weights are likely to aggregate to form micelles at 120 °C.

We estimated the weight percentage of small particles indicative of single polymer chains as 99.97 wt % at 120 °C, using the previously reported method.[25] This result confirmed that the block copolymer aggregation is negligible even at a sufficiently higher temperature than the aggregation temperature. This may be attributed to the weak attractive force between PBnMA chains in the micellar cores. The intermolecular van der Waals attractive interaction appeared to be weak since the PBnMA segment was short ($M_n = 2$ kDa). In addition, the glass transition temperature (T_g) of short PBnMA chain appeared to be lower than the well-known T_g value of PBnMA ($T_g = 54$ °C). The core of the self-assembled aggregates must have been in a rubbery state because the T_g of PBnMA was at least lower by 50 °C than the LCST phase separation temperature of the PBnMA core. Such aggregation behavior is likely to be explained by molecular weight distribution of PBnMA segment. 0.03 wt % of P(BnMA$_{2.2}$-*b*-MMA$_{19}$), which forms the aggregates, may have higher weight ratios of PBnMA than PBnMA/PMMA = 2.2/19.

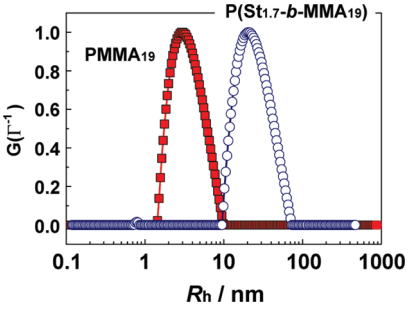

Figure 3. Distribution function of R_h at 25 °C in [C$_2$mim][NTf$_2$] for PMMA$_{19}$ (3 wt %), square, and for P(St$_{1.7}$-*b*-MMA$_{19}$) (1 wt %), circle.

Table 2. R_h Values of P(St$_{1.7}$-*b*-MMA$_{19}$) and PMMA$_{19}$, Measured at 25 °C in Acetone or in [C$_2$mim][NTf$_2$]

	R_h in acetone/nm	R_h in [C$_2$mim][NTf$_2$]/nm
PMMA$_{19}$	3.3	3.5
P(St$_{1.7}$-*b*-MMA$_{19}$)	3.5/59	25

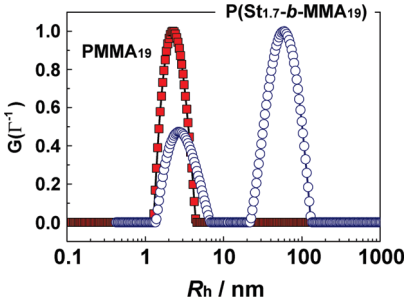

Figure 4. Distribution function of R_h at 25 °C in acetone for PMMA$_{19}$ (2 wt %), square, and for P(St$_{1.7}$-*b*-MMA$_{19}$) (2 wt %), circle.

P(St-*b*-MMA) diblock copolymers have already been reported to form self-assembled structures in an IL, irrespective of temperature.[26] In order to make a comparison of the thermosensitivity and size of aggregates with P(BnMA-*b*-MMA)s in [C$_2$mim][NTf$_2$], P(St$_{1.7}$-*b*-MMA$_{19}$) was designed to have a similar molecular weight and composition to those of P(BnMA$_{2.2}$-*b*-MMA$_{19}$). Figure 3 shows the CONTIN results for P(St$_{1.7}$-*b*-MMA$_{19}$) and the PMMA$_{19}$ precursor in [C$_2$mim][NTf$_2$] at room temperature. In contrast to Figure 2b, a single and intense peak could be observed in both the solutions. The R_h values of the polymer particles calculated from the cumulant fitting for PMMA$_{19}$ and P(St$_{1.7}$-*b*-MMA$_{19}$) at 25 °C are compared in Table 2. The R_h of the P(St$_{1.7}$-*b*-MMA$_{19}$) aggregates, estimated to be 25 nm, clearly indicates spherical micelle formation.[26] In the case of PMMA$_{19}$ in [C$_2$mim][NTf$_2$], the R_h value is consistent with that of a single polymer chain. It is interesting to note that there were two peaks in the acetone indicative of the single polymer chain and block copolymer aggregation of P(St$_{1.7}$-*b*-MMA$_{19}$), as shown in Figure 4, although acetone is considered to be a good solvent for both blocks. However, the weight percentage of the large aggregates of P(St$_{1.7}$-*b*-MMA$_{19}$) could be calculated to be 0.02 wt %.[25] Thus, we could conclude that the number of aggregates for the P(St$_{1.7}$-*b*-MMA$_{19}$)/acetone solution was negligible. The temperature dependency of the R_h values for P(St$_{1.7}$-*b*-MMA$_{19}$) and P(BnMA$_{2.2}$-*b*-MMA$_{19}$) in the IL is plotted as a function of temperature in Figure 5. No R_h temperature dependency can be observed for P(St$_{1.7}$-*b*-MMA$_{19}$) in [C$_2$mim][NTf$_2$],

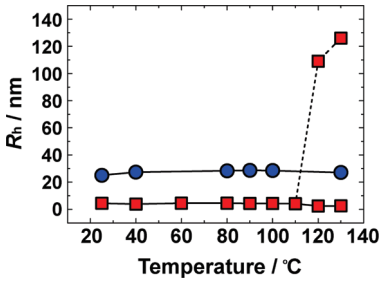

Figure 5. Temperature dependency of R_h in [C_2mim][NTf_2] for P($St_{1.7}$-*b*-MMA_{19}) (1 wt %), circle, and for P($BnMA_{2.2}$-*b*-MMA_{19}) (2 wt %), square. R_h values are estimated by the cumulant (P($St_{1.7}$-*b*-MMA_{19}) at all temperatures and P($BnMA_{2.2}$-*b*-MMA_{19}) below 110 °C) or double-exponential fitting (P($BnMA_{2.2}$-*b*-MMA_{19}) at 120 and 130 °C). Broken line indicates minor components in the system.

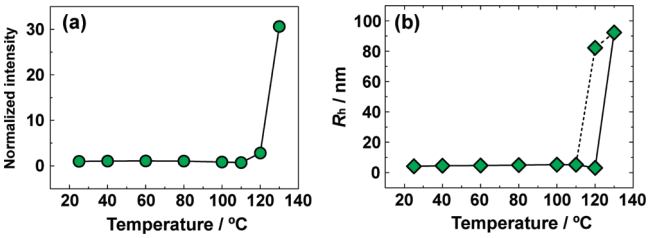

Figure 6. (a) Relationship between the normalized scattering intensity at a scattering angle of 90° and temperature for P($BnMA_{7.3}$-*b*-MMA_{19}) in [C_2mim][NTf_2] solution (2 wt %). Normalized intensity is defined as the intensity at each temperature divided by that measured at 25 °C. (b) Relationship between the R_h of P($BnMA_{7.3}$-*b*-MMA_{19}) in [C_2mim][NTf_2] and the temperature. Broken line indicates minor components in the system.

which is distinctly different from the results of P($BnMA_{2.2}$-*b*-MMA_{19}). The R_h values of the micelles formed by P($St_{1.7}$-*b*-MMA_{19}) increased slightly with an increase in temperature, which could be explained in terms of the extension of the PMMA corona chain and was consistent with a previously reported phenomenon.[26] The size difference between the micelles made by P($BnMA_{2.2}$-*b*-MMA_{19}) and by P($St_{1.7}$-*b*-MMA_{19}) was apparent, although these two diblock copolymers have similar molecular weights and compositions (insoluble block, ca. 2 kDa; soluble block, 19 kDa). The R_h of the aggregates made by P($BnMA_{2.2}$-*b*-MMA_{19}) was 126 nm at 130 °C, whereas the R_h of the micelle by P($St_{1.7}$-*b*-MMA_{19}) was 27 nm. This size difference might come from the difference in the morphology of the micelles. While P($St_{1.7}$-*b*-MMA_{19}) can be judged to form spherical micelles,[26] P($BnMA_{2.2}$-*b*-MMA_{19}) aggregates do not appear to be spherical micelles, but rather worm-like micelles or bilayer vesicles (vide infra).

Aggregation Behavior in an IL of LCMT Diblock Copolymers with Different Molecular Weights and Compositions. P($BnMA_{7.3}$-*b*-MMA_{19}) and P($BnMA_{28}$-*b*-MMA_{41}) were prepared to compare the thermosensitivity of the LCMT diblock copolymers in an IL. Figure 6 shows the normalized scattering intensity and R_h of P($BnMA_{7.3}$-*b*-MMA_{19}) in [C_2mim][NTf_2] (2 wt %). These results also confirmed that P(BnMA-*b*-MMA)s exhibit LCMT aggregation behavior in the IL. The normalized scattering intensity of P($BnMA_{7.3}$-*b*-MMA_{19}) is much larger than that of P($BnMA_{2.2}$-*b*-MMA_{19}) (Figure 1) above the LCMT aggregation temperature.

From the CONTIN analysis for P($BnMA_{7.3}$-*b*-MMA_{19}) in the IL (2 wt %) at 130 °C (Figure 7c), the distribution function appears to correspond to the completely aggregated state of the diblock copolymer. However, as shown in Figure 7b, the distribution function at 120 °C exhibited two peaks, which

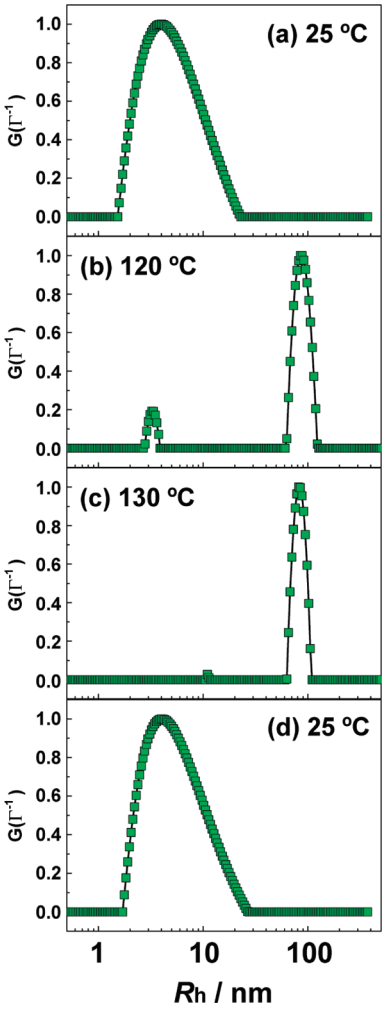

Figure 7. Distribution function of R_h for P($BnMA_{7.3}$-*b*-MMA_{19}) (2 wt %) in [C_2mim][NTf_2] solution measured at (a) 25, (b) 120, and (c) 130 °C during the heating process and then cooled down to (d) 25 °C.

may indicate that the solution was still in the process of aggregation at this temperature. Excellent reversibility between the two morphologies of the polymer in the IL, i.e., the aggregation at high temperatures and the dissociation to unimers at low temperatures, could be observed in the cooling process from 130 to 25 °C (Figure 7c,d). Other P(BnMA-*b*-MMA)s also showed excellent reversibility.

For P($BnMA_{28}$-*b*-MMA_{41}), which had high M_n and f_{BnMA}, the scattering intensity and R_h in the IL are plotted as a function of temperature in parts a and b of Figure 8, respectively. In this case, P($BnMA_{28}$-*b*-MMA_{41}) had completely aggregated at 120 °C. With an increase in the molecular weight of the PBnMA block, the consequent increase in the van der Waals attractive force between the PBnMA chains, which consisted of the micellar cores, resulted in the complete aggregation of P($BnMA_{28}$-*b*-MMA_{41}) at 120 °C. Figure 9 shows the distribution function of P($BnMA_{28}$-*b*-MMA_{41}). A single and sharp peak at 120 °C can be observed at around 100 nm. Table 3 summarizes the R_h values of the P(BnMA-*b*-MMA)s at 25 and 130 °C, calculated from the cumulant or double-exponential fitting. The order of the R_h values for a series of P(BnMA-*b*-MMA)s at 130 °C was P($BnMA_{28}$-*b*-MMA_{41}) (61 nm) < P($BnMA_{7.3}$-*b*-MMA_{19}) (92 nm) < P($BnMA_{2.2}$-*b*-MMA_{19}) (126 nm). These results indicate that the block copolymers with the PBnMA core having the longer polymer chain form a more compact micellar structure.

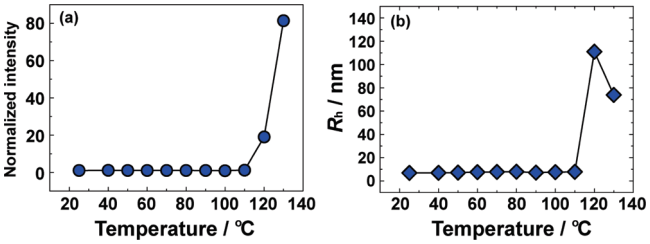

Figure 8. (a) Relationship between the normalized scattering intensity at a scattering angle of 90° and the temperature for P(BnMA$_{28}$-*b*-MMA$_{41}$) in [C$_2$mim][NTf$_2$] solution (2 wt %). Normalized intensity is defined as the intensity at each temperature divided by that measured at 25 °C. (b) Relationship between the R_h of P(BnMA$_{28}$-*b*-MMA$_{41}$) in [C$_2$mim][NTf$_2$] and the temperature.

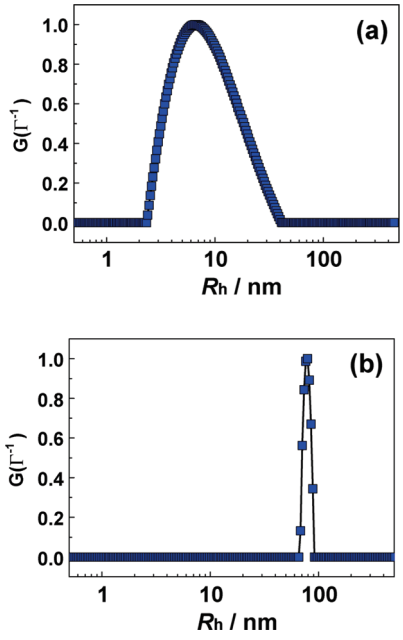

Figure 9. Distribution function of R_h for P(BnMA$_{28}$-*b*-MMA$_{41}$) (2 wt %) in [C$_2$mim][NTf$_2$] solution measured at (a) 25 and (b) 120 °C.

Table 3. R_h Values of Diblock Copolymers in [C$_2$mim][NTf$_2$] Solution (P(St-*b*-MMA), 1 wt %; P(BnMA-*b*-MMA), 2 wt %) Measured at a Low Temperature (25 °C) and at a High Temperature (130 °C)

	R_h/nm (25 °C)	R_h/nm (130 °C)
P(St$_{1.7}$-*b*-MMA$_{19}$)	25	27
P(BnMA$_{2.2}$-*b*-MMA$_{19}$)	4.4	2.5/126
P(BnMA$_{7.3}$-*b*-MMA$_{19}$)	4.2	92
P(BnMA$_{28}$-*b*-MMA$_{41}$)	6.9	61

By making a comparison of aggregation temperatures between P(BnMA-*b*-MMA)s (Figures 1, 6, and 8), it is revealed that the aggregations start at 120 °C for all the block copolymers, although molecular weights of PBnMA segments are significantly different. A similar tendency that the aggregation temperatures (130−140 °C) of acrylamide block copolymers containing PBnMA segments do not change with a change in the molecular weight of PBnMA has been observed in our precious study.[16d] We need further study on this point.

We also need to point out here that the micelles formed by the P(BnMA-*b*-MMA)s were exceptionally large, compared with those of P(St$_{1.7}$-*b*-MMA$_{19}$) (Table 3). The micellar morphology could be varied by tuning the interfacial tension between the solvatophobic blocks and the solvent or by changing the compositions of the block copolymers.[27] The self-assembly of the large aggregates for P(BnMA-*b*-MMA)s appeared to have a different morphology than spherical micelles, for example, bilayer vesicles or cylindrical aggregates. In terms of the interfacial tension between the core block and the IL, we could not find a difference between the P(St$_{1.7}$-*b*-MMA$_{19}$) and the P(BnMA-*b*-MMA)s, since the surface energies of PSt (39 mN/m)[28] and PBnMA (36 mN/m)[28] are nearly equal, and the same IL is used. On the other hand, the volume fraction of the PSt or PBnMA segments ($f_{St,BnMa}$) for P(St$_{1.7}$-*b*-MMA$_{19}$), P(BnMA$_{2.2}$-*b*-MMA$_{19}$), P(BnMA$_{7.3}$-*b*-MMA$_{19}$), and P(BnMA$_{28}$-*b*-MMA$_{41}$) increased from 0.091 to 0.40 (Table 1), which facilitated the formation of cylinders and vesicles in this order. Another possibility would be that the self-assembly of P(St$_{1.7}$-*b*-MMA$_{19}$) did not reach a state of thermal equilibrium, since the solution in the IL was prepared by the cosolvent evaporation method and the PSt core was always below or near its T_g.[29] Lodge et al. correlated the CONTIN distribution function from DLS measurements and the direct visualization of the micellar morphology from the cryo-TEM images for P(B-*b*-EO) self-assembly in an IL.[16b] The structure of the self-assembled micelles in this study will be elucidated in the future by direct observation using electron microscopy techniques.

4. Conclusion

We reported the LCMT aggregation behavior of diblock copolymers in a typical hydrophobic IL, [C$_2$mim][NTf$_2$]. Well-defined P(BnMA-*b*-MMA)s and P(St-*b*-MMA), having different molecular weights and block compositions, were successfully prepared by ATRP. The scattering intensity and R_h values for the polymer particles in the IL were compared between P(BnMA-*b*-MMA)s and P(St-*b*-MMA) as a function of temperature. P(BnMA-*b*-MMA)s were dissolved in the IL as unimers at temperatures below the aggregation temperatures, while they formed large self-assembled aggregates above these temperatures. The transformation between the two states exhibited excellent reversibility. The R_h of the aggregates made by P(BnMA-*b*-MMA)s was much larger than that of P(St-*b*-MMA) (Table 3). For the P(BnMA-*b*-MMA)s, it was reasonable to consider that the aggregates had a different morphology than spherical micelles, such as worm-like micelles or vesicle-like micelles. LCMT aggregation behavior has traditionally been reported in block copolymer aqueous solutions. This is the first example of the LCMT micellization of diblock copolymers in an IL solvent.

Acknowledgment. We gratefully acknowledge the financial support of a Grant-in-Aid for Scientific Research from the MEXT of Japan in the priority area "Science of Ionic Liquids" (#452-17073009) and in the basic research (#B-20350104). K.U. acknowledges the financial support provided by JSPS.

Supporting Information Available: ^{1}H NMR charts and GPC traces for all of the polymers prepared in this study. This material is available free of charge via the Internet at http://pubs.acs.org.

References and Notes

(1) (a) Ueki, T.; Watanabe, M. *Macromolecules* **2008**, *41*, 3739. (b) Winterton, N. *J. Mater. Chem.* **2006**, *16*, 4281. (c) Lodge, T. P. *Science* **2008**, *321*, 50.

(2) (a) Susan, M. A. B. H.; Kaneko, T.; Noda, A.; Watanabe, M. *J. Am. Chem. Soc.* **2005**, *127*, 4976. (b) Seki, S.; Susan, M. A. B. H.; Kaneko, T.; Tokuda, H.; Noda, A.; Watanabe, M. *J. Phys. Chem. B* **2005**, *109*, 3886. (c) Yeon, S. H.; Kim, K. S.; Choi, S.; Cha, J. H.; Lee, H. *J. Phys. Chem. B* **2005**, *109*, 17928.

(3) (a) Tang, J. B.; Tang, H. D.; Sun, W. L.; Plancher, H.; Radosz, M.; Shen, Y. *Chem. Commun.* **2005**, 3325. (b) Tang, J. B.; Tang, H. D.; Sun, W. L.; Radosz, M.; Shen, Y. *Macromolecules* **2005**, *38*, 2037.
(4) (a) Sneddon, P.; Cooper, A. I.; Scott, K.; Winterton, N. *Macromolecules* **2003**, *36*, 4549. (b) Carlin, R. T.; Fuller, J. *Chem. Commun.* **1997**, *15*, 1345.
(5) (a) Swiderski, K.; McLean, A.; Gordon, C. M.; Vaughan, D. H. *Chem. Commun.* **2004**, 2178. (b) Lee, S. H.; Lee, B. B. *Chem. Commun.* **2005**, 3469. (c) Santos, L. M. N. B. F.; Canongia, L. J. N.; Coutinoho, J. A. P.; Esperanca, J. M. S. S.; Gomes, L. R.; Marrucho, I. M.; Rebelo, L. P. N. *J. Am. Chem. Soc.* **2007**, *129*, 284.
(6) Plechkova, N. V.; Seddon, K. R. *Chem. Soc. Rev.* **2008**, *37*, 123.
(7) (a) Swatloski, R. P.; Spear, S. K.; Holbrey, J. D.; Rogers, R. D. *J. Am. Chem. Soc.* **2002**, *124*, 4974. (b) Mouthrop, J. S.; Swatlowski, R. P.; Moyna, G.; Rogers, R. D. *Chem. Commun.* **2005**, 1557.
(8) Xie, J. B.; Li, S. H.; Zhang, S. B. *Green Chem.* **2005**, *7*, 606.
(9) (a) Phillips, D. M.; Drummy, L. F.; Conrady, D. G.; Fox, D. M.; Naik, R. R.; Stone, M. O.; Trulove, P. C.; De Long, H. C.; Mantz, R. A. *J. Am. Chem. Soc.* **2004**, *126*, 14350. (b) Phillips, D. M.; Drummy, L. F.; Naik, R. R.; De Long, H. C.; Fox, D. M.; Trulove, P. C.; Mantz, R. A. *J. Mater Chem.* **2005**, 4206.
(10) Schild, H. G. *Prog. Polym. Sci.* **1992**, *17*, 163.
(11) Ueki, T.; Watanabe, M. *Chem. Lett.* **2006**, *35*, 964.
(12) Ueki, T.; Watanabe, M. *Langmuir* **2007**, *23*, 988.
(13) (a) Ueki, T.; Karino, T.; Kobayashi, Y.; Shibayama, M.; Watanabe, M. *J. Phys. Chem. B* **2007**, *111*, 4750. (b) Kodama, K.; Nanashima, H.; Ueki, T.; Kokubo, H.; Watanabe, M. *Langmuir* **2009**, *25*, 3820.
(14) Tsuda, R.; Kodama, K.; Ueki, T.; Kokubo, H.; Imabayashi, S.; Watanabe, M. *Chem. Commun.* **2008**, 4939.
(15) (a) Alexandridis, P., Lindman, B., Eds. *Amphiphilic Block Copolymers: Self-Assembly and Applications*; Elsevier: Amsterdam, 2000. (b) Howker, C. J.; Wooley, K. L. *Science* **2005**, *309*, 1200. (c) Lodge, T. P.; Bang, J. A.; Li, Z. B.; Hillmyer, M. A.; Talmon, Y. *Faraday Discuss.* **2005**, *128*, 1. (d) Bates, F. *Science* **2003**, *251*, 898. (e) Hanley, K. J.; Lodge, T. P. *Macromolecules* **2000**, *33*, 5918.
(16) (a) Anderson, J. L.; Pino, V.; Hagberg, E. C.; Sheares, V. V.; Armstrong, D. W. *Chem. Commun.* **2003**, 2444. (b) He, Y.; Li, Z.; Simone, P.; Lodge, T. P. *J. Am. Chem. Soc.* **2006**, *128*, 2745. (c) Patrascu, C.; Gauffre, F.; Nallet, F.; Bordes, R.; Oberdisse, J.; L-Viguerie, N.; Mingotaud, C. *Chem. Phys. Chem.* **2006**, *7*, 99. (d) Ueki, T.; Watanabe, M.; Lodge, T. P. *Macromolecules* **2009**, *42*, 1315.
(17) He, Y.; Boswell, P. G.; Buhlmann, P.; Lodge, T. P. *J. Phys. Chem. B* **2007**, *111*, 4645.
(18) (a) He, Y.; Lodge, T. P. *Chem. Commun.* **2007**, 2732. (b) He, Y.; Lodge, T. P. *Macromolecules* **2008**, *41*, 167.
(19) (a) He, Y.; Lodge, T. P. *J. Am. Chem. Soc.* **2006**, *128*, 12666. (b) Bai, Z.; He, Y.; Lodge, T. P. *Langmuir* **2008**, *24*, 5284. (c) Bai, Z.; He, Y.; Young, N. P.; Lodge, T. P. *Macromolecules* **2008**, *41*, 6615.
(20) Simone, P.; Lodge, T. P. *Macromolecules* **2008**, *41*, 1753.
(21) (a) Hajduk, D. A.; Kossuth, M. B.; Hillmyer, M. A.; Bates, F. S. *J. Phys. Chem. B* **1998**, *102*, 4269. (b) Meradovic, D.; van Nostrum, C. F.; Hennink, W. E. *Macromolecules* **2001**, *34*, 7589. (c) Dimitrov, I.; Trzebicka, B.; Müller, A. H. E.; Dworak, A.; Tsvetanov, C. B. *Prog. Polym. Sci.* **2007**, *32*, 1275.
(22) (a) Matyjaszewski, K.; Xia, J. *Chem. Rev.* **2001**, *101*, 2921. (b) Kamigaito, M.; Ando, T.; Sawamoto, M. *Chem. Rev.* **2001**, *101*, 3689.
(23) (a) Noda, A.; Hayamizu, K.; Watanabe, M. *J. Phys. Chem. B* **2001**, *105*, 4603. (b) Tokuda, H.; Tsuzuki, S.; Susan, M. A. B. H.; Hayamizu, K.; Watanabe, M. *J. Phys. Chem. B* **2006**, *110*, 19593.
(24) Queffelec, J.; Gaynor, S. G.; Matyjaszewski, K. *Macromolecules* **2000**, *33*, 8629.
(25) Shibayama, M.; Karino, T.; Okabe, S. *Polymer* **2006**, *47*, 6446.
(26) Simone, P.; Lodge, T. P. *Macromol. Chem. Phys.* **2007**, *208*, 339.
(27) Abbas, S.; Li, Z.; Hassan, H.; Lodge, T. P. *Macromolecules* **2007**, *40*, 4048.
(28) *Polymer Handbook*, 4th ed.; Brandrup, J., Immergut, E. H., Grulke, E. A., Eds.; Wiley-Interscience: Hoboken, NJ, 1999.
(29) Meli, L.; Lodge, T. P. *Macromolecules* **2009**, *42*, 580.